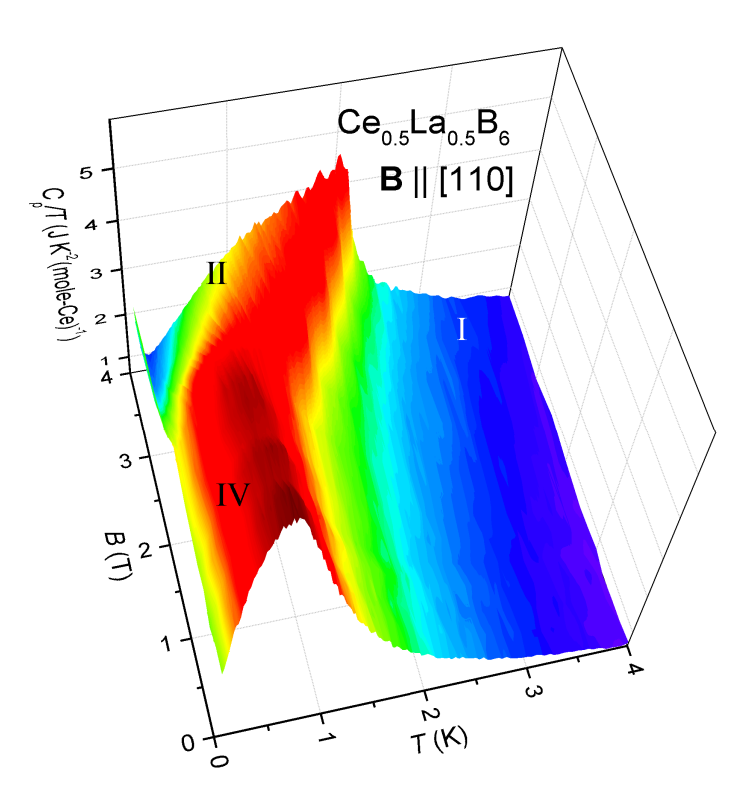
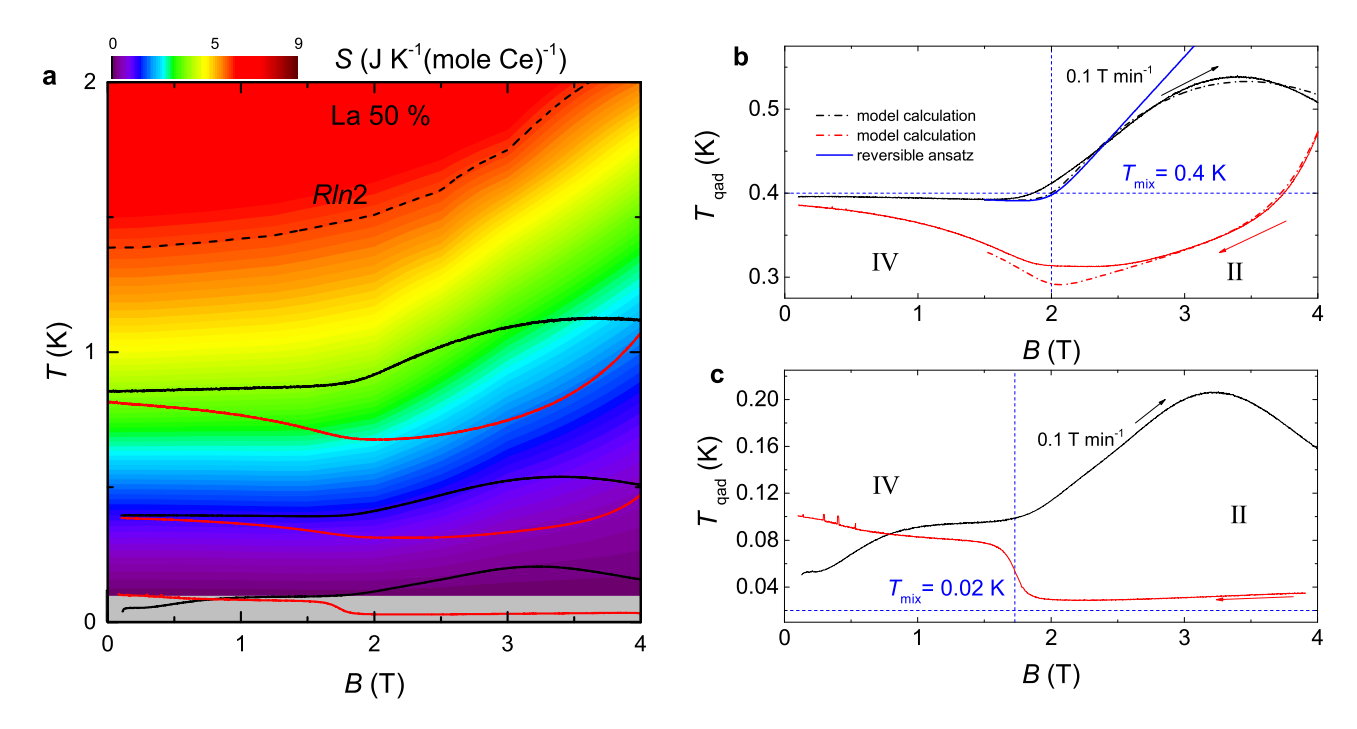
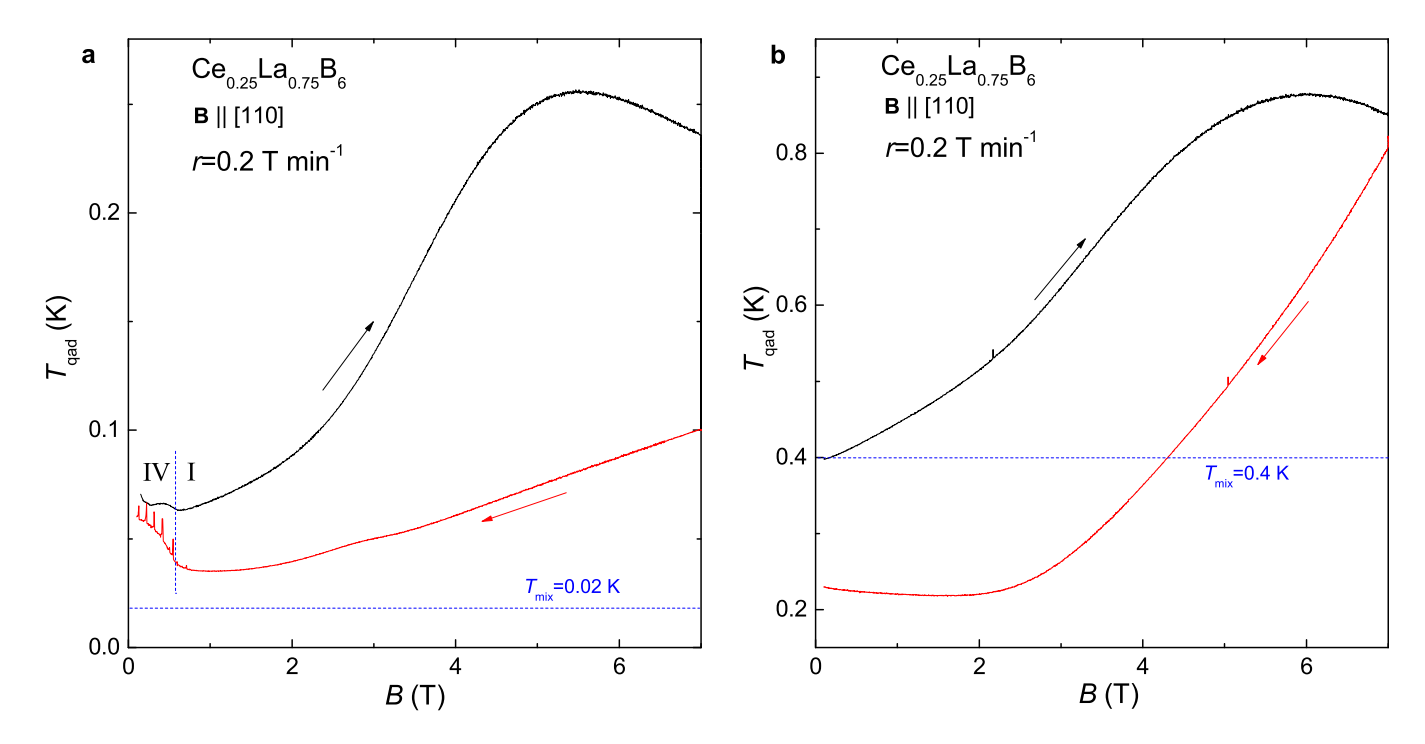
Supplementary Figures



Supplementary Figure 1: Surface plot of the specific heat capacity divided by temperature obtained from $\mathbf{Ce}_{0.5}\mathbf{La}_{0.5}\mathbf{B}_{6}$. External magnetic field is applied along [110] direction and regions of phases I, II, and IV are briefly noted.



Supplementary Figure 2: Quasi-adiabatic MCE in $Ce_{0.5}La_{0.5}B_6$ superimposed on the contour plot of its entropy. a, Representative $T_{\rm qad}(B)$ curves with $T_{\rm mix}=0.02$ K, 0.4 K, and 0.8 K are shown. For a reference, $S_p=R\ln 2$ line is inserted with the black dashed-line and the background is the contour plot of the entropy. Black and red solid-lines are results for increasing and decreasing field, respectively. b, $T_{\rm qad}(B)$ curves with $T_{\rm mix}=0.4$ K are displayed. The model calculations without field-induced heating are exhibited with dash-dotted lines. The blue vertical dashed-line is placed to demarcate phase II-IV transition. c, $T_{\rm qad}(B)$ curves with $T_{\rm mix}=0.02$ K are displayed. The blue vertical dashed-line is placed where $|dT_{\rm qad}(B)/dB|$ is the largest in down-sweep. The sweep-rate is 0.1 T min⁻¹ in all panels.



Supplementary Figure 3: Quasi-adiabatic MCE observed in $Ce_{0.25}La_{0.75}B_6$. a, Black and red solid-lines are $T_{\rm qad}(B)$ curves with increasing and decreasing field, respectively. The temperature of the mixing chamber $T_{\rm mix}$ is 0.02 K. The blue vertical dashed line marks the phase transition between phase I and phase IV. b, Curves for the quasi-adiabatic temperature $T_{\rm qad}(B)$ are shown at $T_{\rm mix}=0.4$ K. The sweep-rate is 0.2 T min⁻¹ in both panels.

Supplementary Notes

Supplementary Note 1

Surface plot of the specific heat capacity of $Ce_{0.5}La_{0.5}B_6$ divided by the temperature: Specific heat capacity under constant pressure and field, $C_{p,B}$, of $Ce_{0.5}La_{0.5}B_6$ is measured as a function of temperature. The values of the external magnetic field are from 0 T to 4 T with 0.25 T interval. Then, the obtained $C_{p,B}(T)$ curves compose the frame of the interpolated surface plot. Field-insensitive peaks around 1 K and below 2.5 T are clearly shown and we suspect these peaks indicate rather broadened phase transition between phase I and phase IV. As the field is further increased, phase IV is suppressed and phase II emerges. This can be recognized by the field-induced $(1/2 \ 1/2 \ 1/2)$ Bragg intensity (refer to Ref. 37 in the main text). The phase transition is not very clear in 2D plots but these are more distinguishable in the 3D plot.

Supplementary Note 2

Analysis of the quasi-adiabatic MCE: Here, we derive the differential equation for the theoretical quasi-adiabatic temperature, $T_{\rm qad}^0(B)$. First, we consider a term for the reversible (equilibrium) MCE, and then add a term which reflects an excessive field-induced heating. Given that the specimen with a virtual temperature $T_{\rm qad}^0$ is linked to the mixing chamber at the temperature of $T_{\rm mix}$, there should also be a term representing a natural relaxation of $T_{\rm qad}^0$ to $T_{\rm mix}$. Taking pieces together, we can express the general differential equation with respect to $dT_{\rm qad}^0/dB$ as

$$\frac{dT_{\text{qad}}^0}{dB} = \frac{dT_{\text{rev}}}{dB} \pm \frac{dT_{\text{irr}}^{\pm}}{dB} \mp \frac{1}{|r|C_p(T,B)} \int_{T_{\text{mix}}}^{T_{\text{qad}}^0} dTK(T,B), \tag{1}$$

where the double signs are in the same order and the equation with the upper (lower) sign is applicable for the situation with increasing (decreasing) field. $dT_{\rm rev}$ is an infinitesimal temperature change following an isentropic line. $dT_{\rm irr}^{\pm}$ is an infinitesimal temperature change due to a field-induced heating other than the eddy current heating. It is quantitatively discussed in the last paragraph of the current section that the eddy current heating is negligible. The thermal conduction coefficient K(T,B) between the sample and the mixing chamber is extracted by analyzing the relaxation of $T_{\rm qad,B}(t)$ to the $T_{\rm mix}$, and we found $K(T,B) = \alpha T^{\delta}$ with negligible B-dependence below 5 T. Here, $\alpha \simeq 100$ nW K⁻¹ and $\delta = 1.2$. r in the last term is field sweep-rate.

By experience, we already know that many of analytic expressions for thermodynamic functions are written in various combinations of hyperbolic functions. Hence, using $T_{\rm rev} \propto \{\tanh(B-B_{\rm c})+1\}$ is a good starting point to construct a reversible ansatz for the MCE since this function well depicts stepwise temperature change upon the phase transition. Here, $|dT_{\rm qad}^0/dB|$ is the largest at an arbitrary critical field $B_{\rm c}$. We further elaborate this idea to imitate isentropic lines calculated in the main text with the following expression,

$$T_{\text{rev}}(B_{\text{f}}) = C_{1}^{\text{rev}} \left\{ \tanh(w_{1}^{\text{rev}}(B_{\text{f}} - B_{\text{c}})) + 1 \right\} + \frac{C_{2}^{\text{rev}}}{w_{2}^{\text{rev}}} \ln \left| \frac{\cosh\{w_{2}^{\text{rev}}(B_{\text{f}} - B_{\text{c}})\}}{\cosh\{w_{2}^{\text{rev}}(B_{\text{i}} - B_{\text{c}})\}} \right| + w_{3}^{\text{rev}} C_{2}^{\text{rev}}(B_{\text{f}} - B_{\text{i}}), \tag{2}$$

where C_1^{rev} determines the size of the stepwise temperature change in a narrow range of field close to B_c , and w_1^{rev} determines sharpness of the transition. Behavior of isentropic lines in a wider range of field are determined by adjusting C_2^{rev} , w_2^{rev} , and w_3^{rev} . B_i and B_f are the initial and the final fields for the eq. (1), respectively. In this way, all the blue curves for the reversible ansatz in Fig. 4 of the main text are generated.

The irreversible temperature change is approximated by the following function,

$$T_{\rm irr}^{\pm}(B) = \sum_{i=1}^{2} D_i^{\pm} \{ \tanh(w_i^{\pm}(B - B_i^{\pm}) + 1 \}.$$
 (3)

The envelopes of red-filled and black-hatched areas in Fig. 4 of the main text are described by the relation $dQ/dB \simeq C_p(T_{\rm qad},B)dT_{\rm irr}^\pm(B)/dB$.

Finally, eqs. (2) and (3) are implanted in eq. (1) and numerically solved for $T_{\rm qad}^0(B)$. The parameters in eqs. (2) and (3) are iteratively adjusted until the $T_{\rm qad}^0(B)$ is optimized to the $T_{\rm qad}(B)$. It should be emphasized that more than two hyperbolic terms in eq. (3) do not improve the quality of the numerical estimation. Also, note that we

are dealing with only the second order phase transition because the ansatz for the equilibrium MCE is continuous and reversible. Here, we do not enumerate values of parameters but summarize specific conditions which are unique to different of phase boundaries. In case $B_1^+=B_2^+=B_1^-=B_2^-=B_c$ and $D_i^+=D_i^-$, the heating curves are reversible. II-III' transitions are well described by this condition. When $B_1^+=B_2^+\neq B_1^-=B_2^-$ and $D_i^+=D_i^-$ AFM structural phase transitions around III-III' boundaries are well reproduced. In case $B_1^+=B_2^+\neq B_1^-=B_2^-$ and $D_i^+\neq D_i^-$, the dQ/dB curves can have different shapes depending on the sweep direction. With this condition, we can describe highly hysteretic features in $T_{\rm qad}(B)$.

It is suggested that an intensive scattering of quasiparticles triggered by strongly fluctuating local moments could be the major cause of the irreversible $T_{\rm qad}(B)$ in the vicinity of a phase transition. We designate this kind of field-induced heating as the critical heating. The magnitude of the heating due to the domain motion, which we define as the domain heating, is usually much smaller than the magnitude of the critical heating. Also, the domain heating is not concentrated in a narrow range around a phase boundary. It is well represented in Fig. 4b of the main text that, although the domain heating is easily distinguishable in phase III', $T_{\rm qad}(B)$ is monotonically increasing over wide the range of field.

Assuming a cylindrical geometry of radius R, height L, power dissipation per unit volume by the eddy current is given by $P/V = E_{\phi}(R)^2/2\rho = R^2(\partial B_z/\partial t)^2/8\rho$. The field is along the z-direction. Taking the average dimension of the specimen R=L=1 mm and the resistivity $\rho \simeq 10~\mu\Omega$ cm, 0.26 nJ of eddy current heating $Q_{\rm eddy}$ is generated for 40 min with r=0.1 T min⁻¹. At 0.1 K, the heat capacity, C, of 5 mg of CeB₆ is 0.37 μ JK⁻¹. Putting the estimated values together, the temperature increase $\Delta T = Q_{\rm eddy}/C$ becomes 0.7 mK for 40 min in a perfectly adiabatic condition. It is definitely negligible compared to notable changes in $T_{\rm qad}(B)$.

Supplementary Note 3

Critical points determined by quasi-adiabatic MCE in $Ce_{1-x}La_xB_6$ with x=0.5 and 0.75: At x=0.5, the quasi-adiabatic MCE shows a broad transition feature between phase II and phase IV except at very low T below 0.05 K (Supplementary Figure 2a). For $T_{\rm mix}=0.4$ K, eq. (3) is solved without a critical heating and solutions are superimposed with dash-dotted lines as shown in the Supplementary Figure 2b. The steepest slope of the reversible ansatz is assumed to appear at the critical field as noted by the vertical blue dashed-line. On the other hand, the critical heating strongly affects the $T_{\rm qad}(B)$ at very low T: see the down-sweep in the Supplementary Figure 2c. In this case, the numerical calculation is very difficult because we cannot estimate correct values for $C_p(T,B)$ below 0.05 K. The critical point is located where $|dT_{\rm qad}(B)/dB|$ has the largest slope (see the vertical dashed line in Supplementary Figure. 2c). It is conjectured that the MC sweep correctly captures intensive fluctuations of order parameters in the vicinity of a critical point noted in Fig. 5c of the main text.

Supplementary Figure 3 exhibits $T_{\rm qad}(B)$ curves in Ce_{0.25}La_{0.75}B₆. When the mixing chamber is anchored to 0.02 K (Supplementary Figure 3a), we observe the critical heating below 0.8 T and the star-shaped symbol in Fig. 5c of the main text is referenced to this value. We deduce that the quantum fluctuation regarding the I-IV phase transition at 0.8 T is detected by the MC sweep. This statement is strongly supported by the observation of the maximum in γ_0 at the same field (Fig. 5b of the main text). In addition, it must be noted that there exists a subtle wiggling in $T_{\rm qad}(B)$ around 3.5 T below 0.05 K. This is suspected as reminiscent of the weak I-II transition. As the system is away from T=0, the critical heating is no longer observed and only a paramagnetic response remains (Supplementary Figure 3b). The spikes in the red curve is due to the flux jump from the superconducting magnet.